RESEARCH PAPER

Effective fabrication of poly(anilin-formaldehyde)-supported hybrid nanomaterial and catalytic synthesis of dihydropyridines

Mohammad Ali Bodaghifard [1,2], Zahra Faraki[1], Sajad Asadbegi[1]*

[1] Department of Chemistry, Faculty of Science, Arak University, Iran

[2] Institute of Nanosciences and Nanotechnology, Arak University, Arak, Iran

ARTICLE INFO

ABSTRACT

In this study, $Fe_3O_4@SiO_2$-PAF-SO_3H nanocomposite was successfully fabricated by immobilization of sulfonic acid groups on the surface of poly(anilin-formaldehyde)-supported on magnetic $Fe_3O_4@SiO_2$ nanoparticles through layer-by-layer assembly. The $Fe_3O_4@SiO_2$-PAF-SO_3H composite nanostructure was fully characterized using various techniques including Fourier-transform infrared spectroscopy (FT-IR), X-ray powder diffraction patterns (XRD), thermogravimetric analysis (TGA), scanning electron microscopy (SEM), energy dispersive X-ray spectroscopy (EDS) and vibrating sample magnetometry (VSM). The one-pot synthesis of mono and bis 1,4-dihydropyridine derivatives, as pharmaceutically interesting compounds, were achieved in high yields via three-component and pseudo-five-component condensation of an aromatic aldehyde, ammonium acetate and ethyl acetoacetate in the presence of $Fe_3O_4@$ SiO_2-PAF-SO_3H as a novel retrievable hybrid nanocatalyst under solvent-free conditions. This protocol has advantages in terms of short reaction time, solvent-free condition, high yield and purity, easy work-up and eco-friendly process as well as recyclability of the nanocatalyst (at least 6 times) with no decrease in catalytic activity.

INTRODUCTION

Magnetic nanoparticles (MNPs) attract great attention of worldwide scientist and researchers because of their ripsnorting distinguished properties such as high surface area, low cost, low toxicity, high stability, simple separation, easy synthesis and functionalization [1-3]. Due to the unique and valuable properties of MNPs, several applications and potential activities have been reported for MNPs in the field of electronic, biology, pharmacology, drug delivery and catalysis area [3-5]. The heterogenization of homogeneous acidic and basic groups in catalytic reactions (such as covalently bound acidic or basic catalysts) allows for the facile separation and reuse of catalysts. The inorganic-supported catalysts especially hybrid magnetic nanomaterials, inorganic-polymer hybrid nanocomposites have been widely used in recent years that could be applied in diverse applications such as drug delivery system, catalysis and biological diagnostics [3, 6-8].

In multicomponent reactions (MCRs), several available compounds (three or more starting materials) react simultaneously in one container to result a desired product. MCRs produce complex and diverse combinations of products and follow many principles of green chemistry, such as solvent-free or aqueous condition, atom economy, energy saving with short reaction times, waste diminish, high yields and selectivity [9-12]. The

* Corresponding Author Email: *mbodaghi2007@yahoo.com*
m-bodaghifard@araku.ac.ir
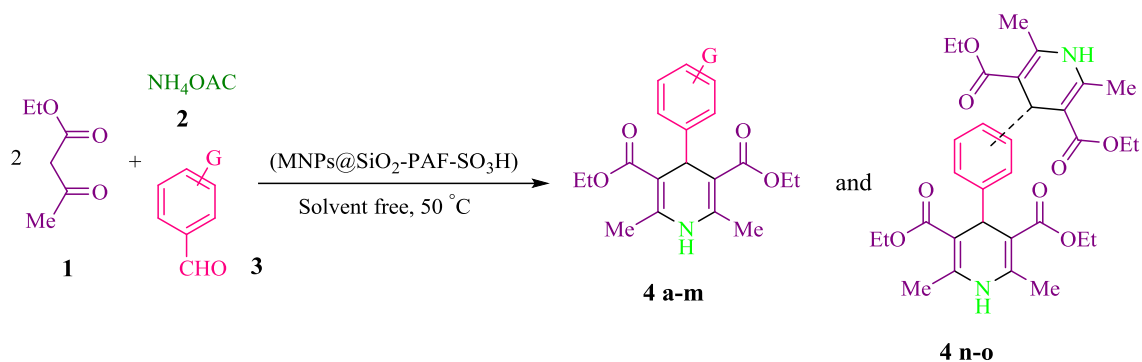
Scheme 1. Synthesis of 1,4-dihydropyridine derivatives using novel $Fe_3O_4@SiO_2$-PAF-SO_3H as a catalyst.

1,4-dihydropyridine derivatives are known as an important group of heterocyclic compounds having a special place in organic chemistry due to their extensive pharmaceutical activities [13,14]. These compounds have many therapeutic treatments as sedative, anti-hypertensive [15,16], anticonvulsant [17], calcium channel blockers [18-21] and anti-clot treatment [22,23]. Many reported synthetic methods for 1,4-dihydropyridine suffer from limitations such as low efficiency, long reaction time, the use of toxic solvents, the use of expensive catalysts, difficult reaction conditions and boring purification procedures. To overcome some of these obstacles, we have synthesized a novel magnetic hybrid nanocatalyst, namely $Fe_3O_4@SiO_2$-PAF-SO_3H, and investigated its role as an efficient catalyst for synthesize of 1,4-dihydropyridine derivatives via the one-pot three-component and pseudo five component condensation of an aromatic aldehyde, ammonium acetate and ethyl acetate under solvent-free condition (Scheme 1).

EXPERIMENTAL SECTION
Materials and methods
The chemicals were purchased from reputable chemical companies (Merck, Aldrich, and Fluka) or were synthesized and purified in the laboratory. The FT-IR spectra were recorded using a Galaxy-series FT-IR 5030 spectrophotometer in the region 4000–400 cm^{-1} using pressed KBr Discs. The ^1H and ^{13}C-NMR spectra were recorded on a Brucker Avance spectrometer operating at 300 MHz for ^1H and 75 MHz for ^{13}C-NMR in DMSO-d_6 with TMS as an internal standard. Powder X-ray diffraction (XRD) was carried out using a Philips XPert (Cu-Kα radiation, λ = 0.15405 nm) over the range $2q$ = 20–80° using 0.04° as the step length. Thermal gravimetric analysis (TGA) and differential

thermal gravimetric (DTG) data for $Fe_3O_4@SiO_2$-PAF-SO_3H MNPs were recorded on a Mettler TA4000 System under an atmosphere of N_2 at a heating rate of 10 °C min^{-1}. The magnetization and hysteresis loop were measured at room temperature using a Vibrating Sample Magnetometer (Model 7300 VSM system, Lake Shore Cryotronic, Inc., Westerville, OH, USA). The scanning electron microscope measurement was carried out using a Hitachi S-4700 field emission-scanning electron microscope (FE-SEM). The transmission electron microscopy (TEM) measurements were performed on a Philips CM10 analyzer operating at 150 kV.

Synthesis of $Fe_3O_4@SiO_2$-PAF-SO_3H hybrid nano-material
Fe_3O_4 nanoparticles were prepared by chemical co-precipitation method described in the literature [24]. The synthesized Fe_3O_4 MNPs were used for coating with a silica shell according to the Stober method [25]. Aminopropyl-modified silica-coated MNPs were prepared according to a reported procedure [26] .In a typical procedure, 1.0 g of $Fe_3O_4@SiO_2$ MNPs was dispersed in 40 mL of dry toluene using an ultrasonic bath for 30 minutes to produce a uniform suspension. Then, 0.6 mL of 3-aminopropyltriethoxysilane (APTES) was added using a syringe. The reaction mixture was refluxed under N_2 atmosphere at 110 °C for 12 h. Finally, the aminopropyl-functionalized solid ($Fe_3O_4@SiO_2$–PrNH₂ MNPs) was washed with toluene for several times, separated using a magnet, and dried under vacuum. To synthesize $Fe_3O_4@SiO_2$-PAF-NH₂, a mixture of 1 g of formaldehyde, 0.5 g of aniline and 1 g of $Fe_3O_4@SiO_2$–PrNH₂ in 50 mL of DMF at 100 ml round-bottomed flask was stirred under sonication. Then, the mixture was stirred with a magnetic stirrer for 24 h at 100 °C. After

the reaction was completed, the precipitate was washed several times with hot ethanol and dried in an oven. In the last step, 1 g of Fe_3O_4@SiO_2-PAF-NH_2 in 40 mL dichloromethane was stirred for 10 minutes, then by placing the reaction mixture under aqueous vacuum 1 g of chlorosulfonic acid was added slowly and the reaction mixture was stirred at room temperature for 2 h. The resulting precipitate was washed with ethanol and dried in the vacuum oven to result in the final hybrid acidic nanomaterial (Fe_3O_4@SiO_2-PAF-SO_3H).

General procedure for the synthesis of 1,4-dihydropyridines

A mixture of an aromatic aldehyde (1 mmol), ammonium acetate (3 mmol, 60 mg) (in an excess amount), ethyl acetoacetate (2 mmol, 0.254 ml), and Fe_3O_4@SiO_2-PAF-SO_3H (0.02 g) was magnetically stirred under the thermal solvent-free condition on a preheated oil bath at 50 °C for an appropriate time. The progress of the reaction was monitored by TLC. After completion of the reaction, the resulting solidified mixture was diluted with hot ethanol (10 mL) and the catalyst was easily separated by an external magnet and reused for the subsequent runs. Water was added to the remaining clear solution, after which the precipitate was appeared and separated. The pure, crystalline 1,4-dihydropyridine was achieved by crystallization in a mixture of ethanol : water (1:1).

Selected spectroscopic data

4a: IR (KBr) (n_{max}, cm^{-1}): 3344, 3063, 2982, 1689, 1653, 1489, 1375, 1213, 1091. ^{1}H NMR (DMSO-d_6, 300 MHz) d$_H$: 1.47 (6H, t, CH$_3$ (OCH$_2$CH$_3$), J= 5.4 Hz), 2.27 (6H, s, CH$_3$), 4.02 (4H, q, CH$_2$ (OCH$_2$CH$_3$) J=5.4 Hz), 4.92 (1H, s, CH), 5.48 (1H, s, NH), 7.01-7.24 (4H, m, H$_{arom}$).

4b: IR (KBr) (n_{max}, cm^{-1}): 3358, 2989, 1697, 1653, 1487, 1371, 1215, 1093. ^{1}H NMR (DMSO-d_6, 300 MHz) d$_H$: 1.13 (6H, t, CH$_3$ (OCH$_2$CH$_3$), J= 5.4 Hz), 2.20 (6H, s, CH$_3$), 4.02 (4H, q, CH$_2$ (OCH$_2$CH$_3$) J=5.4 Hz), 4.92 (1H, s, CH), 6.30 (1H, s, NH), 7.05-7.16(4H, m, H$_{arom}$).

4c: IR (KBr) (n_{max}, cm^{-1}): 3352, 3090, 2980, 1653, 1595, 1477, 1373, 1217, 1081. ^{1}H NMR (DMSO-d_6, 300 MHz) d$_H$: 1.15 (6H, t, CH$_3$ (OCH$_2$CH$_3$), J= 5.1 Hz), 2.21 (6H, s, CH$_3$), 4.01 (4H, q, CH$_2$ (OCH$_2$CH$_3$) J=5.1 Hz), 4.89 (1H, s, CH), 6.23 (1H, br, NH), 7.04-7.15 (4H, m, H$_{arom}$).

4e: IR (KBr) (n_{max}, cm^{-1}): 3348, 3094, 2984, 1693, 1566, 1500, 1373, 1213, 1099. ^{1}H NMR (DMSO-d_6, 400 MHz) d$_H$: 1.15 (6H, t, CH$_3$ (OCH$_2$CH$_3$), J= 5.1 Hz), 2.23 (6H, s, CH$_3$), 3.95 (4H, q, CH$_2$ (OCH$_2$CH$_3$) J=5.1 Hz), 4.86 (1H, s, CH), 6.58-7.05 (4H, m, H$_{arom}$), 7.99(1H, s, OH and NH).

4g: IR (KBr) (n_{max}, cm^{-1}): 3346, 2991, 1647, 1527, 1487, 1348, 1213, 1118. ^{1}H NMR (DMSO-d_6, 400 MHz) d$_H$: 1.24 (6H, t, CH$_3$ (OCH$_2$CH$_3$), J= 5.1 Hz), 2.37 (6H, s, CH$_3$), 4.08 (4H, q, CH$_2$ (OCH$_2$CH$_3$) J=5.4Hz), 5.10 (1H, s, CH), 5.63 (1H, s, NH), 7.44-8.09 (4H, m, H$_{arom}$).

4j: IR (KBr) (n_{max}, cm^{-1}): 3340, 3095, 2984, 2837, 1689, 1614, 1491, 1373, 1303, 1028. ^{1}H NMR (DMSO-d_6, 300 MHz) d$_H$: 1.23 (6H, t, CH$_3$ (OCH$_2$CH$_3$), J= 5.1 Hz), 2.33 (6H, s, CH$_3$), 3.76 (3H, s, OCH$_3$), 4.10 (4H, q, CH$_2$ (OCH$_2$CH$_3$) J=5.1 Hz), 4.93 (1H, s,CH), 5.54 (1H, s, NH), 6.74-7.22 (4H, m, H$_{arom}$).

4l: IR (KBr) (n_{max}, cm^{-1}): 3354, 2976, 2841, 1693, 1604, 1570, 1504, 1371, 1275, 1207, 1124. ^{1}H NMR (DMSO-d_6, 300 MHz) d$_H$: 1.19 (6H, t, CH$_3$ (OCH$_2$CH$_3$), J= 5.4 Hz), 2.31 (6H, s, CH$_3$), 3.82 (3H, s, OCH$_3$), 4.06 (4H, q, CH$_2$ (OCH$_2$CH$_3$) J=5.4 Hz), 4.97 (1H, s, CH), 6.28 (1H, s, NH and OH), 6.43-6.91 (4H, m, H$_{arom}$).

4n: IR (KBr) (n_{max}, cm^{-1}): 3364, 3092, 2986, 2841, 1682, 1620, 1491, 1371, 1305, 1222, 1030. ^{1}H NMR (DMSO-d_6, 300 MHz) d$_H$: 1.11 (12H, t, CH$_3$ (OCH$_2$CH$_3$), J= 5.1 Hz), 2.23 (12H, s, CH$_3$), 3.95 (8H, q, CH$_2$ (OCH$_2$CH$_3$) J=5.1 Hz), 4.76 (2H, s, CH), 6.95 (4H, s, H$_{arom}$), 8.75 (2H, s, NH).

4o: IR (KBr) (n_{max}, cm^{-1}): 3340, 3163, 2984, 1691, 1491, 1371, 1303, 1211, 1114. ^{1}H NMR (DMSO-d_6, 300 MHz) d$_H$: 1.09 (12H, t, CH$_3$ (OCH$_2$CH$_3$), J= 5.4 Hz), 2.23 (12H, s, CH$_3$), 3.95 (8H, q, CH$_2$ (OCH$_2$CH$_3$) J=5.4 Hz), 4.79 (2H, s, CH), 6.85- 6.99 (4H, m, H$_{arom}$), 8.75 (2H, s, NH).

RESULTS AND DISCUSSION

Characterization of novel Fe_3O_4@SiO_2-PAF-SO_3H catalyst

The Fe_3O_4@SiO_2-PAF-SO_3H catalyst was prepared as shown in Scheme 2. Fourier transform infrared (FT-IR) spectroscopy, X-ray diffraction (XRD), field emission scanning electron microscopy (FE-SEM), energy dispersive X-ray spectroscopy (EDS), thermogravimetric analysis (TGA) and vibrating sample magnetometry (VSM) were used to identify and characterize the prepared catalyst.

The FT-IR spectra of Fe_3O_4, Fe_3O_4@SiO_2, Fe_3O_4@SiO_2-NH_2, Fe_3O_4@SiO_2-PAF-NH_2 and Fe_3O_4@SiO_2-PAF-SO_3H are shown in Fig. 1. The FT-IR spectrum
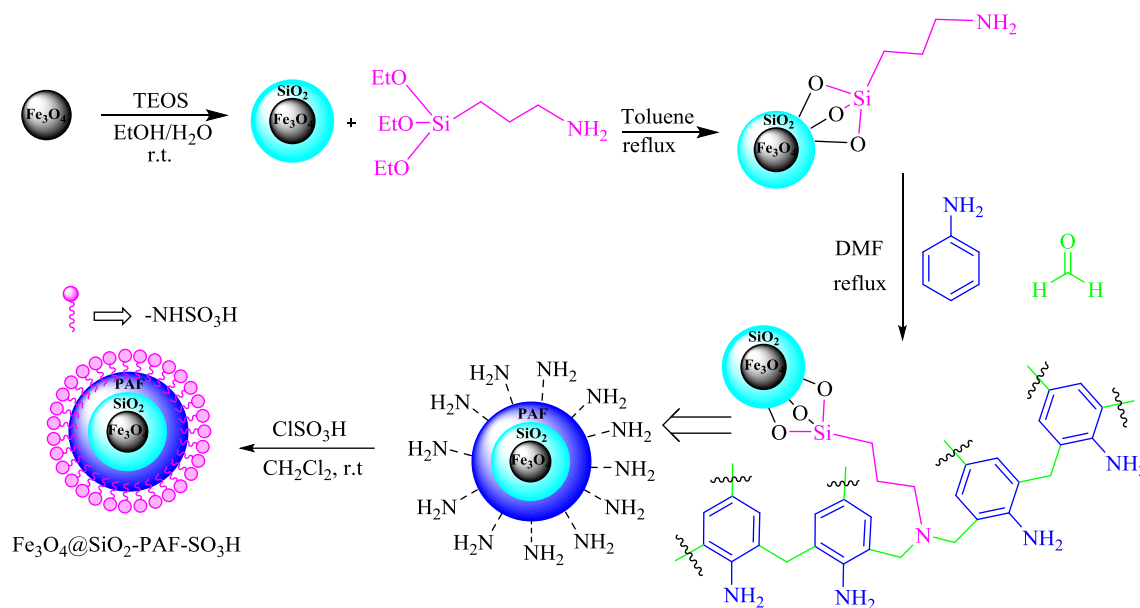
Scheme 2. The sequential steps for preparation of $Fe_3O_4@SiO_2$-PAF-SO_3H as a novel hybrid nanomaterial
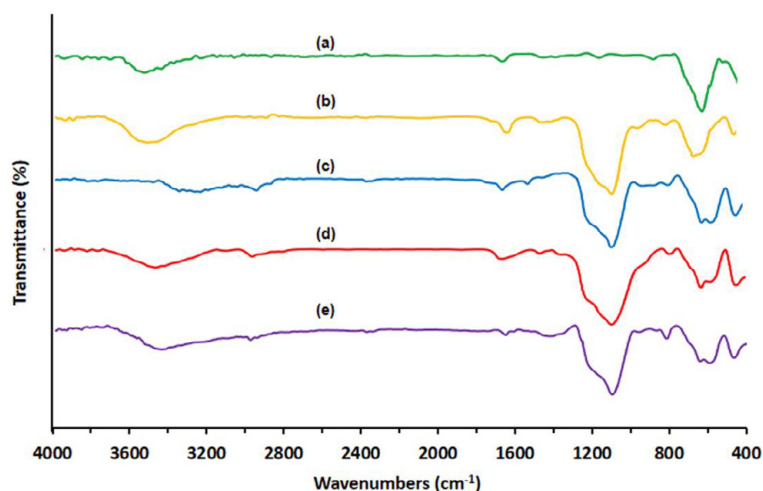
Fig. 1. Comparison of FT-IR spectra for (a) Fe_3O_4, (b) $Fe_3O_4@SiO_2$, (c) $Fe_3O_4@SiO_2$-NH_2, (d) $Fe_3O_4@SiO_2$-PAF-NH_2 and (e) $Fe_3O_4@SiO_2$-PAF-SO_3H

of magnetic Fe_3O_4 MNPs shows the characteristic Fe–O absorption band around 580 cm^{-1} (Fig. 1a). $Fe_3O_4@SiO_2$ shows characteristic FT-IR bands at around 1100 cm^{-1}, 950 cm^{-1}, 820 cm^{-1} and 460 cm^{-1} which are attributed to the asymmetric stretching, symmetric stretching, in plane bending and rocking mode of the Si–O–Si group, respectively, that confirm the formation of SiO_2 shell. The broad peak observed in the range of 3200 - 3500 cm^{-1} was related to the stretching vibration mode of Si-OH and H-O-H. The weak peak located in 1630 cm^{-1} was due to the O–H stretching vibration mode of

Si–OH. The weak bands at 2920 cm^{-1} and 2960 cm^{-1} were related to the C-H symmetric and asymmetric stretching modes of the attached alkyl groups (Fig 1c-e). Thus, the obtained results indicate that the functional groups were successfully grafted onto the surface of the magnetic nanoparticles.

The XRD analysis result confirmed the presence as well as the degree of crystallinity of magnetic Fe_3O_4 and the $Fe_3O_4@SiO_2$-PAF-SO_3H catalyst (Fig. 2). The same peaks were observed in both of the Fe_3O_4 and $Fe_3O_4@SiO_2$-PAF-SO_3H patterns, demonstrating retention of the crystalline spinel

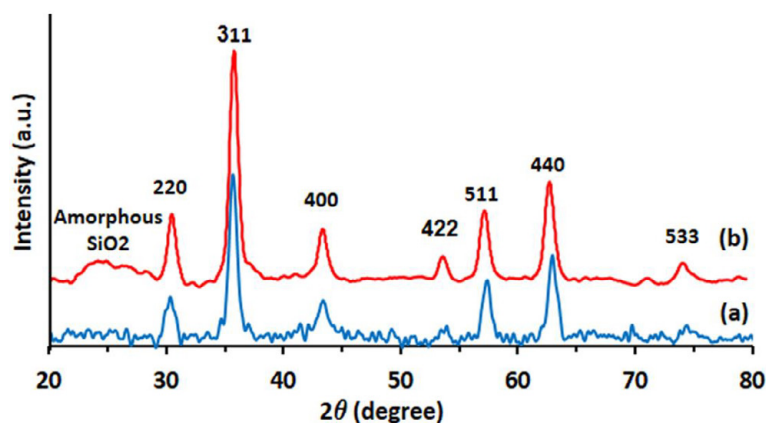Fig. 2. XRD patterns of (a) Fe_3O_4 MNPs and (b) Fe_3O_4@SiO_2-PAF-SO_3H
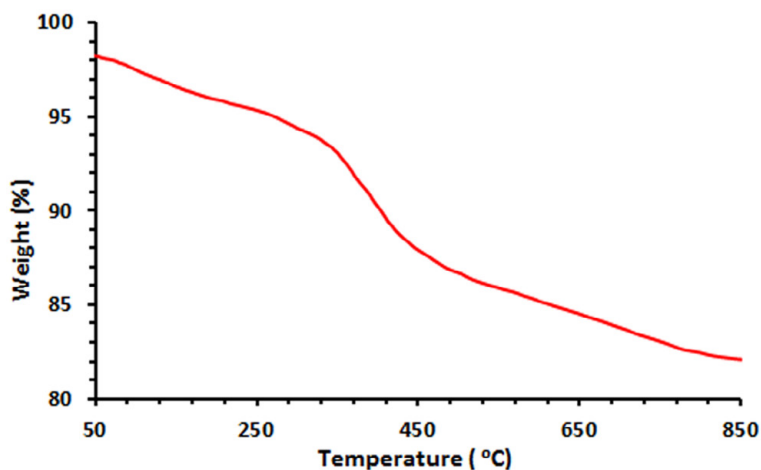

Fig. 3. TGA for Fe_3O_4@SiO_2-PAF-SO_3H nanoparticles

ferrite core structure during the coating process. The XRD patterns of the synthesized MNPs exhibit diffraction peaks at $2\theta = 30°$, $35.7°$, $43.3°$, $53.9°$, $57°$, $63.5°$ and $74.5°$ which can be referred to the (220), (311), (400), (422), (511), (440) and (533) planes of Fe_3O_4, respectively. These results indicate that the Fe_3O_4 particles in the nanoparticles are pure Fe_3O_4 with a cubic spinel structure and matched well with the standard Fe_3O_4 sample (JCPDS card no. 85-1436). The broad peak from $2\theta = 22°$ to $28°$ is consistent with an amorphous silica phase of Fe_3O_4@SiO_2-PAF-SO_3H (Fig. 4b). The average crystallite size of MNPs by Scherrer's formula ($D=0.9\lambda/\beta \cos \theta$) was estimated from the (311) XRD peak. The crystallite size of MNPs calculated from the width of the peak at $2\theta = 35.7°$ (311) is 57 nm, which is in the range determined using FE-SEM analysis (Fig. 4).

The stability of the Fe_3O_4@SiO_2-PAF-SO_3H nanocomposite was determined by thermogravimetric analysis (TGA) (Fig. 6). The magnetic catalyst shows two weight loss steps over the temperature range of TGA. (Fig. 3). The first stage, including a low amount of weight loss at T < 300 °C, was due to the removal of physically adsorbed solvent, water and surface hydroxyl groups. The second step at about 300 °C to nearly 600 °C is attributed to the decomposition of the organic layer in the nanocomposite. Therefore, the weight loss between 300 and 600 °C gives the organic moiety ratios grafted on the prepared nanomaterial. The organic moiety grafted on the Fe_3O_4@SiO_2-PAF-SO_3H was approximately 10 wt.%.

FE-SEM was used to investigate the size and morphology of the Fe_3O_4@SiO_2-PAF-SO_3H

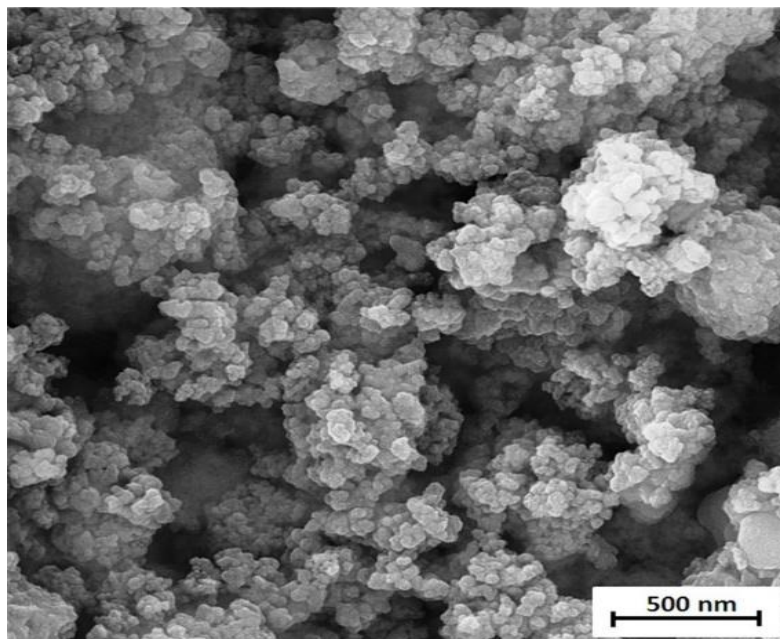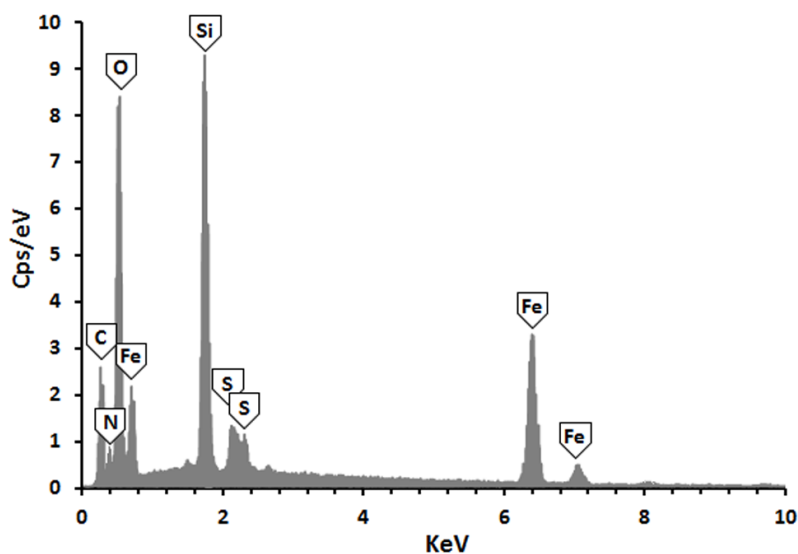Fig. 4. FE-SEM image of $Fe_3O_4@SiO_2$-PAF-SO_3H nanoparticles

Fig. 5. The EDS spectrum of $Fe_3O_4@SiO_2$-PAF-SO_3H nanoparticles

particles (Fig. 4). As can be seen from Fig. 2(a), $Fe_3O_4@SiO_2$-PAF-SO_3H nanoparticles have a mean diameter of about 51 nm and a nearly spherical shape. The EDS analysis obviously shows the presence of N and C in the $Fe_3O_4@SiO_2$-PAF-SO_3H nanoparticles (Fig. 5). Furthermore, the presence of Si, O and Fe signals indicates that the iron oxide particles were loaded into silica, and the higher intensity of the Si peak compared to the Fe peak exhibits that the Fe_3O_4 nanoparticles have been trapped by the SiO_2 layer. So, based on the results, the $Fe_3O_4@SiO_2$-PAF-SO_3H nanocomposite has been fabricated successfully.

The magnetic properties of the nanoparticles was distinguished using a vibrating sample magnetometer (VSM). Fig. 6 shows the plots of
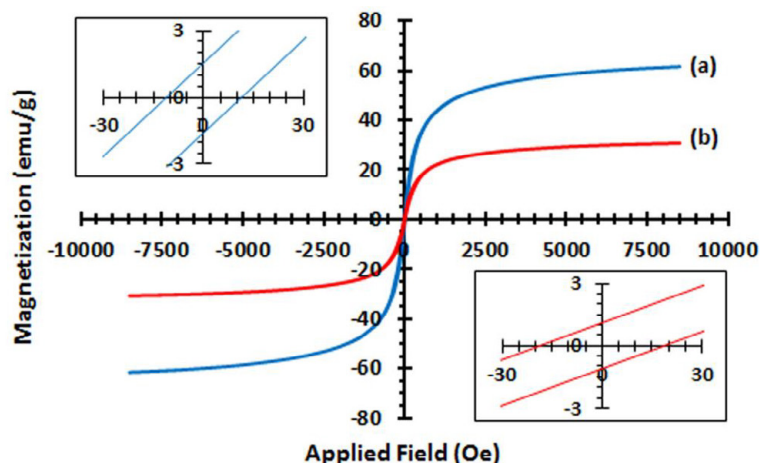
Fig. 6. Magnetic hysteresis loops of (a) Fe_3O_4 MNPs and (b) Fe_3O_4@SiO_2-PAF-SO_3H Left-hand inset: magnified view from -20 to 20 Oe.

Table 1. Optimization of reaction conditions for preparation of 1,4-dihydropyridine derivatives.
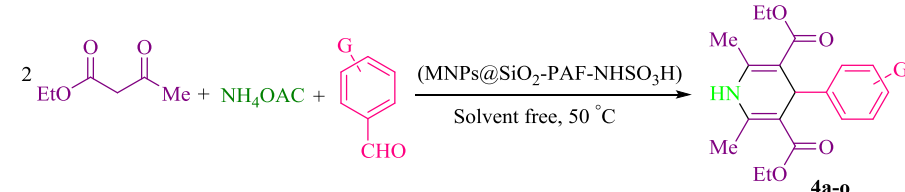

No.	Catalyst (mg)	Solvent	Temp (°C)	Time (h)	Yield (%) [a]
1	Fe_3O_4@SiO_2-PAF-SO_3H (10)	-	80	5	78
2	Fe_3O_4@SiO_2-PAF-SO_3H (20)	-	80	2	93
3	Fe_3O_4@SiO_2-PAF-SO_3H (30)	-	80	2	90
4	Fe_3O_4@SiO_2-PAF-SO_3H (20)	EtOH	80	2	80
5	Fe_3O_4@SiO_2-PAF-SO_3H (20)	H_2O	80	2	76
6	Fe_3O_4@SiO_2-PAF-SO_3H (20)	EtOH-H_2O (2 : 1)	80	2	68
7	Fe_3O_4@SiO_2-PAF-SO_3H (20)	CH_3Cl	80	2	57
8	Fe_3O_4@SiO_2-PAF-SO_3H (20)	CH_3CN	80	2	57
9	Fe_3O_4@SiO_2-PAF-SO_3H (20)	CH_3CO_2Et	80	2	65
10	Fe_3O_4@SiO_2-PAF-SO_3H (20)	-	50	1	95
11	Fe_3O_4@SiO_2-PAF-SO_3H (20)	-	60	2	91
12	Fe_3O_4@SiO_2-PAF-SO_3H (20)	-	100	2	85
13	Fe_3O_4@SiO_2-PAF-SO_3H (20)	-	r.t	8	50
14	Fe_3O_4 (20)	-	50	2	30
15	Fe_3O_4@SiO_2 (20)	-	50	2	35
16	Fe_3O_4@SiO_2-PAF-NH_2 (20)	-	50	2	38
17	-	-	50	2	23

[a] isolated yields.

room temperature magnetization (M) versus magnetic field (H) (M–H curves or hysteresis loops) of Fe_3O_4 and Fe_3O_4@SiO_2-PAF-SO_3H nanoparticles. The hysteresis curve allows determination of the saturation magnetization (Ms), remanent magnetization (Mr) and coercivity (Hc). The magnetization of samples could be completely saturated at high fields up to ±8000.0

Table 2. Multicomponent one-pot synthesis of 1,4-dihydropyridines.

Product	Ar	Time (h)	Yield (%)[a]	MP (°C)[b]	
				Found	Reported
4a	C_6H_5	1.2	90	156	157-159 [28]
4b	4-Cl-C_6H_4	1	95	152-153	149 [28]
4c	3-Cl-C_6H_4	1	91	224-225	-
4d	4-Me-C_6H_4	1.2	92	156-158	158-160 [28]
4e	4-OH-C_6H_4	1.5	90	222-224	226-228 [28]
4f	3-OH-C_6H_4	1.5	89	184-185	180-182 [28]
4g	4-NO_2-C_6H_4	1	93	127	129-131 [28]
4h	3-NO_2-C_6H_4	1	90	162-163	161-163 [28]
4i	2-NO_2-C_6H_4	1	91	171-173	169-170 [28]
4j	4-OMe-C_6H_4	1	93	155-157	158-160 [28]
4k	2-OMe-C_6H_4	1	93	142-144	141-143 [28]
4l	4-OH-3-OMe-C_6H_4	1.2	90	160-162	162 [29]
4m	2-pyridyl	1	90	189-191	192-194 [30]
4n[c]	4-CHO-C_6H_4	1.5	90	235-237	-
4o[c]	3-CHO-C_6H_4	1.5	92	230-232	-

[a] Isolated yields

[b] Melting points were not corrected.

[c] 4 mmol ethyl acetoacetate, 4 mmol ammonium acetate and 1 mmol aldehyde were used and bis-dihydropyridine as products were obtained.

Oe and, due to the formation of a silica shell around the Fe3O4 core, the Ms of samples changes from 57.8 to 33.4 emu g^{-1} The hysteresis loops exhibit the super-paramagnetic behavior of the Fe_3O_4 and Fe_3O_4@SiO_2-PAF-SO_3H particles in which the Mr and Hc are close to zero (Mr = 0.85 and 0.45 emu per g, and Hc = 4.90 and 4.0 Oe, respectively) [27].

Synthesis of 1,4-dihydropyridines catalyzed by Fe_3O_4@SiO_2-PAF-SO_3H

The 4-chlorobenzaldehyde, ammonium acetate and ethyl acetoacetate were selected as model substrates and the reaction was carried out in various conditions to obtain the optimized condition. The different solvents as well as solvent-free medium, temperatures and catalyst amounts were examined on model reaction and the results are shown in Table 1. Under the solvent free condition, and use of 20 mg of Fe_3O_4@SiO_2-PAF-SO_3H as a catalyst at 50 °C, serves as the best condition with respect to the green nature and clean workup procedure for this synthesis (Table 1, entry 10). To define the role of Fe_3O_4@SiO_2-PAF-SO_3H as a catalyst for the

preparation of 1,4-dihydropyridines, the model reaction was performed under the same conditions with Fe_3O_4, Fe_3O_4@SiO_2, Fe_3O_4@SiO_2-PAF-NH_2, Fe_3O_4@SiO_2-PAF-SO_3H and without any catalyst. With respect to the reaction time and yield of product, the best results are achieved using Fe_3O_4@SiO_2-PAF-SO_3H as the catalyst (Table 1, entry 10, 14-17). In order to determine the generality and efficacy of the catalyst, various aldehydes carrying either electron-donating or electron-withdrawing groups were reacted under the optimized reaction condition. It was found that the reactions for all of the various substrates proceed efficiently to produce corresponding 1,4 dihydropyridine in good to excellent yields without formation of side products (Table 2). A possible mechanism for the construction of 1,4-dihydropyridine is shown in Scheme 3. Fe_3O_4@SiO_2-PAF-SO_3H as an acidic catalyst activates the carbonyl group and facilitates the condensation reactions. Firstly, Knoevenagel condensation of aldehyde and β-ketoester takes place to form intermediate I. Then, intermediate II is produced by the condensation of the second
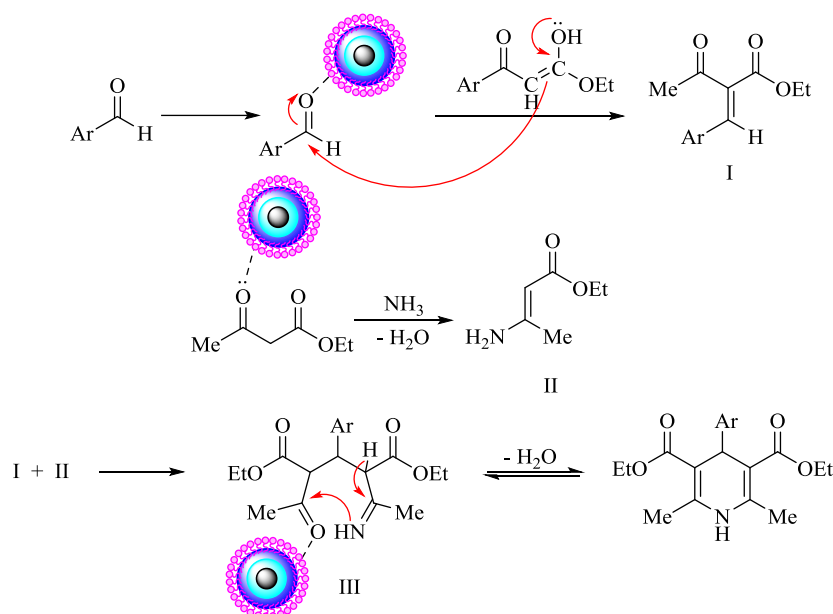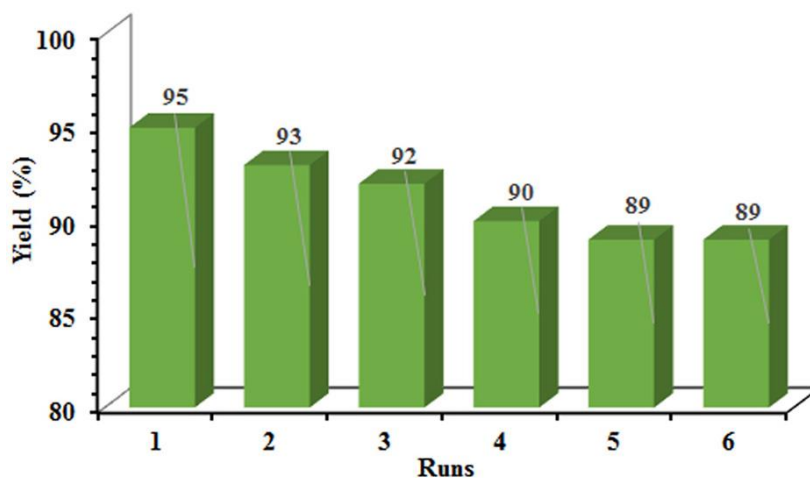
Scheme 3: Possible mechanism for the synthesis of 1,4-dihydropyridines using $Fe_3O_4@SiO_2$-PAF-SO_3H

Fig. 7. Recyclability of MNPs-AQ in the preparation of 1,4-dihydropyridines.

equivalent of β-ketoester. Finally, condensation of these two fragments results in intermediate III, which subsequently is cyclized (intramolecular) to the target product in the presence of the catalyst and with elimination of H_2O molecule (Scheme 3).

Catalyst recovery and reuse

The recovery and reusability of the catalyst are very important for commercial and industrial applications as well as green process aspects. Thus,

the recovery and reusability of $Fe_3O_4@SiO_2$-PAF-SO_3H was investigated in the model reaction. After completion of the reaction, the resulting solidified mixture was diluted with hot EtOH (15 mL). Then, the catalyst was easily separated, washed with hot EtOH, dried under vacuum and reused in a subsequent reaction. Nearly, quantitative recovery of catalyst (up to 97%) could be obtained from each run. As seen in Fig. 7, the recycled catalyst could be reused six times without any additional treatment

or appreciable reduction in catalytic activity. The consistent structure and activity of recovered and reused $Fe_3O_4@SiO_2$-PAF-SO_3H catalyst confirms its stability, recyclability and performance for the synthesis of desired heterocycles.

CONCLUSION

In summary, a layer of poly aniline-formaldehyde was fabricated on magnetic nanoparticles surfaces and functionalized by sulfonic acid groups successfully. The novel magnetic inorganic-polymer hybrid nanostructure ($Fe_3O_4@SiO_2$-PAF-SO_3H) was characterized and successfully applied as an acidic retrievable nanocatalyst for preparation of mono and bis 1,4-dihydropyridine derivatives in high yields via three-component and pseudo-five-component condensation reaction. This protocol has advantages in terms of short reaction time, solvent-free condition, high yield and purity, easy work-up and eco-friendly process as well as the recyclability of the nanocatalyst with no notable diminish in catalytic performance.

ACKNOWLEDGEMENTS

CONFLICT OF INTEREST
The authors declare that they have no conflict of interest.

REFERENCES
1. Polshettiwar V, Luque R, Fihri A, Zhu H, Bouhrara M, Basset J-M. Magnetically Recoverable Nanocatalysts. Chemical Reviews. 2011;111(5):3036-75.
2. Shylesh S, Schünemann V, Thiel WR. Magnetically Separable Nanocatalysts: Bridges between Homogeneous and Heterogeneous Catalysis. Angewandte Chemie International Edition. 2010;49(20):3428-59.
3. Bodaghifard MA, Hamidinasab M, Ahadi N. Recent Advances in the Preparation and Application of Organic– inorganic Hybrid Magnetic Nanocatalysts on Multicomponent Reactions. Current Organic Chemistry. 2018;22(3):234-67.
4. Sau TK, Rogach AL, Jäckel F, Klar TA, Feldmann J. Properties and Applications of Colloidal Nonspherical Noble Metal Nanoparticles. Advanced Materials. 2010;22(16):1805-25.
5. Wu D-Y, Liu X-M, Huang Y-F, Ren B, Xu X, Tian Z-Q. Surface Catalytic Coupling Reaction of p-Mercaptoaniline Linking to Silver Nanostructures Responsible for Abnormal SERS Enhancement: A DFT Study. The Journal of Physical Chemistry C. 2009;113(42):18212-22.
6. Minakata S, Komatsu M. Organic Reactions on Silica in Water. Chemical Reviews. 2009;109(2):711-24.
7. Kitanosono T, Masuda K, Xu P, Kobayashi S. Catalytic Organic Reactions in Water toward Sustainable Society.

Chemical Reviews. 2017;118(2):679-746.
8. Narayanan R, El-Sayed MA. Catalysis with Transition Metal Nanoparticles in Colloidal Solution: Nanoparticle Shape Dependence and Stability. The Journal of Physical Chemistry B. 2005;109(26):12663-76.
9. Jiménez-Alonso S, Chávez H, Estévez-Braun A, Ravelo ÁG, Feresin G, Tapia A. An efficient synthesis of embelin derivatives through domino Knoevenagel hetero Diels–Alder reactions under microwave irradiation. Tetrahedron. 2008;64(37):8938-42.
10. Dömling A. Isocyanide based multi component reactions in combinatorial chemistry. Comb Chem High Throughput Screen. 1998;1(1):1-22.
11. Dömling A, Ugi I. Multicomponent Reactions with Isocyanides. Angewandte Chemie. 2000;39(18):3168-210.
12. Nair V, Rajesh C, Vinod AU, Bindu S, Sreekanth AR, Mathen JS, et al. Strategies for Heterocyclic Construction via Novel Multicomponent Reactions Based on Isocyanides and Nucleophilic Carbenes. Accounts of Chemical Research. 2003;36(12):899-907.
13. Bajaj SD, Mahodaya OA, Tekade PV. ZSM-5 Catalyzed Solvent Free Ecofriendly Synthesis of Substituted Pyrimidine Derivatives. Pharmaceutical Chemistry Journal. 2015;48(10):679-82.
14. Schnell B, Strauss UT, Verdino P, Faber K, Kappe CO. Synthesis of enantiomerically pure 4-aryl-3,4-dihydropyrimidin-2(1 H)-ones via enzymatic resolution: preparation of the antihypertensive agent (R)-SQ 32926 †Synthesis and reactions of Biginelli compounds, part 20; for part 19, see: Kappe, C. O.; Shishkin, O. V.; Uray, G.; Verdino, P. Tetrahedron 2000, 56, 1859–1862. †. Tetrahedron: Asymmetry. 2000;11(7):1449-53.
15. Gaudio AC, Korolkovas A, Takahata Y. Quantitative Structure-Activity Relationships for 1,4-Dihydropyridine Calcium Channel Antagonists (Nifedipine Analogues): A Quantum ChemicalKlassical Approach. Journal of Pharmaceutical Sciences. 1994;83(8):1110-5.
16. Schleifer K-J. Stereoselective Characterization of the 1,4-Dihydropyridine Binding Site at L-Type Calcium Channels in the Resting State and the Opened/Inactivated State. Journal of Medicinal Chemistry. 1999;42(12):2204-11.
17. Khadilkar B, Borkar S. Silica Gel Supported Ferric Nitrate: A Convenient Oxidizing Reagent. Synthetic Communications. 1998;28(2):207-12.
18. Schnell B, Krenn W, Faber K, Kappe CO. Synthesis and reactions of Biginelli-compounds. Part 23. Chemoenzymatic syntheses of enanttiomerically pure 4-aryl-3,4-dihydropyrimidin-2(1H)-ones. Journal of the Chemical Society, Perkin Transactions 1. 2000(24):4382-9.
19. Janis RA, Triggle DJ. New developments in calcium ion channel antagonists. Journal of Medicinal Chemistry. 1983;26(6):775-85.
20. Boecker RH, Guengerich FP. Oxidation of 4-aryl- and 4-alkyl-substituted 2,6-dimethyl-3,5-bis(alkoxycarbonyl)-1,4-dihydropyridines by human liver microsomes and immunochemical evidence for the involvement of a form of cytochrome P-450. Journal of Medicinal Chemistry. 1986;29(9):1596-603.
21. Gordeev MF, Patel DV, Gordon EM. Approaches to Combinatorial Synthesis of Heterocycles: A Solid-Phase Synthesis of 1,4-Dihydropyridines. The Journal of Organic Chemistry. 1996;61(3):924-8.

22. Pattan SR, Rasal VP, Venkatramana NV, Khade AB, Butle SR, Jadhav SG, et al. Synthesis and Evaluation of Some 1,4-Dihydropyridine and Their Derivatives as Antihypertensive Agents. ChemInform. 2007;38(32).

23. Suresh T, Swamy SK, Reddy VM. Synthesis and Bronchodilatory Activity of New 4-Aryl-3,5-bis (2-chlorophenyl)carbamoyl-2,6-dimethyl-1,4-dihydropyridines and Their 1-Substituted Analogues. ChemInform. 2007;38(22).

24. Chen F, Xie S, Zhang J, Liu R. Synthesis of spherical Fe3O4 magnetic nanoparticles by co-precipitation in choline chloride/urea deep eutectic solvent. Materials Letters. 2013;112:177-9.

25. Morel A-L, Nikitenko SI, Gionnet K, Wattiaux A, Lai-Kee-Him J, Labrugere C, et al. Sonochemical Approach to the Synthesis of Fe3O4@SiO2 Core−Shell Nanoparticles with Tunable Properties. ACS Nano. 2008;2(5):847-56.

26. Moghanian H, Mobinikhaledi A, Blackman AG, Sarough-Farahani E. Sulfanilic acid-functionalized silica-coated magnetite nanoparticles as an efficient, reusable and magnetically separable catalyst for the solvent-free synthesis of 1-amido- and 1-aminoalkyl-2-naphthols. RSC Adv. 2014;4(54):28176-85.

27. Petcharoen K, Sirivat A. Synthesis and characterization of magnetite nanoparticles via the chemical co-precipitation method. Materials Science and Engineering: B. 2012;177(5):421-7.

28. Tamaddon F, Ghazi S. Urease: A highly biocompatible catalyst for switchable Biginelli reaction and synthesis of 1,4-dihydropyridines from the in situ formed ammonia. Catalysis Communications. 2015;72:63-7.

29. Sharma P, Gupta M. Silica functionalized sulphonic acid coated with ionic liquid: an efficient and recyclable heterogeneous catalyst for the one-pot synthesis of 1,4-dihydropyridines under solvent-free conditions. Green Chemistry. 2015;17(2):1100-6.

30. Tamaddon F, Razmi Z, Jafari AA. Synthesis of 3,4-dihydropyrimidin-2(1H)-ones and 1,4-dihydropyridines using ammonium carbonate in water. Tetrahedron Letters. 2010;51(8):1187-9.